water

MDPI

Article

Integrated Struvite Precipitation and Fenton Oxidation for Nutrient Recovery and Refractory Organic Removal in Palm Oil Mill Effluent

Yi Fen Sea, Adeline Seak May Chua, Gek Cheng Ngoh and Mohamad Fairus Rabuni *

Sustainable Process Engineering Centre (SPEC), Department of Chemical Engineering, Faculty of Engineering, Universiti Malaya, Kuala Lumpur 50603, Malaysia; yifen@um.edu.my (Y.F.S.)
* Correspondence: fairus.rabuni@um.edu.my

Abstract: Anaerobically treated palm oil mill effluent (AnT-POME), containing a high concentration of ammoniacal-nitrogen (NH_4^+-N) and soluble chemical oxygen demand (sCOD) was subjected to sequential processes of struvite precipitation to recover NH_4^+-N and Fenton oxidation for sCOD removal. The optimization of treatment was conducted through response surface methodology (RSM). Under optimized struvite precipitation conditions (Mg^{2+}/NH_4^+, PO_4^{3-}/NH_4^+ molar ratios: 1; pH 8.2 ± 0.1), NH_4^+-N concentration decreased to 41 ± 7.1 mg L^{-1} from an initial 298 ± 41 mg L^{-1} (78.8 ± 1.6 % removal). Field emission scanning electron microscopy (FESEM) coupled with energy-dispersive X-ray spectroscopy (EDX) confirmed NH_4^+-N was recovered as struvite. Subsequent Fenton oxidation under the optimized conditions (H_2O_2 dosage: 2680 mg L^{-1}; molar ratio of Fe^{2+}/H_2O_2: 0.8; reaction time: 56 min) reduced sCOD concentration to 308 ± 46 mg L^{-1} from an initial 1350 ± 336 mg L^{-1} (76.0 ± 1.0 % removal). The transparent appearance of treated AnT-POME validated the removal of sCOD responsible for the initial brownish appearance. Models derived from RSM demonstrated significance, with high coefficients of determination (R^2 = 0.99). Overall, integrated struvite precipitation and Fenton oxidation effectively removed NH_4^+-N and sCOD from AnT-POME, contributing to nutrient recovery and environmental sustainability.

Keywords: agro-industrial waste; circular economy; NH_4^+-N removal; response surface methodology; sCOD removal

Citation: Sea, Y.F.; Chua, A.S.M.; Ngoh, G.C.; Rabuni, M.F. Integrated Struvite Precipitation and Fenton Oxidation for Nutrient Recovery and Refractory Organic Removal in Palm Oil Mill Effluent. *Water* **2024**, *16*, 1788. https://doi.org/10.3390/w16131788

Academic Editor: Daniel Mamais

Received: 10 May 2024
Revised: 8 June 2024
Accepted: 21 June 2024
Published: 25 June 2024

1. Introduction

In the dynamic landscape of the global oil and fats market, the year 2021 witnessed palm oil production emerging as a cornerstone, with Indonesia and Malaysia leading the charge [1]. While the palm oil industry plays a significant role in socio-economic development, the increased mass production of palm oil has inherently led to elevated waste generation, particularly in the form of palm oil mill effluent (POME). POME is recognized for its potential to cause environmental pollution owing to its high biochemical oxygen demand (BOD), chemical oxygen demand (COD), total nitrogen (TN) and total suspended solids (TSS) levels. In general, the BOD, COD, TN and TSS contents are in the ranges of 6418–51,510, 42,500–250,000, 154–2050 and 3115–59,350 mg L^{-1}, respectively [2]. This wastewater is considered high strength, presenting a significant risk to the environment due to its elevated organic content, which can lead to oxygen depletion in water bodies, and its abundant nutrients content, which can contribute to eutrophication. Therefore, it is imperative to implement proper treatment measures before discharging this wastewater into the environment safely.

The conventional ponding system is the prevalent approach in use and consists of a series of biological treatment stages, including anaerobic and aerobic processes. The anaerobic treatment process has demonstrated significant efficacy in the removal of biodegradable

pollutants (i.e., BOD), as reported by Yacob et al. [3]. However, to meet stringent environmental safety standards, subsequent polishing treatment is recommended for anaerobic ponds to enhance the effluent quality. Despite the role of the aerobic ponding system in polishing anaerobically treated POME (AnT-POME), the final effluent is still characterized by its brownish appearance, attributed to the presence of refractory organics such as lignin, tannins, and humic acid [4], which results in elevated COD levels. These refractory organics can impede biological reactions, occasionally causing the final discharge following aerobic treatment sometimes to fall short of discharge standards. A persistent brownish appearance serves as an indicator of pollution. Moreover, while aerobic treatment can efficiently oxidize ammonium (NH_4^+) to nitrate via nitrification, a circular economy approach calls for resource recovery from wastewater by recovering NH_4^+ for other useful uses. Recognizing the limitations of the conventional aerobic ponding system, there is a growing interest in exploring alternative methods of polishing treatment to recover a valuable resource (e.g., NH_4^+) and eliminate COD. Methods such as coagulation, adsorption and membrane technology have been applied to address the pollution potential of POME; however, these methods often fail to eliminate the brownish color associated with COD, requiring additional treatment and limiting nutrient recovery [4].

In the contemporary approach to wastewater treatment, the focus has shifted from mere pollutant removal to resource recovery. One well-known method for nutrient recovery is struvite precipitation, where nutrients in wastewater, specifically NH_4^+ and phosphate (PO_4^{3-}) are precipitated as struvite crystals in an alkaline environment. Within the ponding system, anaerobic treatment has effectively stabilized the organic contents by converting them into carbon dioxide and methane, while also producing NH_4^+ from organic nitrogen through ammonification [5]. The latter serves as a valuable nitrogen source for plant nutrition, underscoring the importance of struvite precipitation in removing and recovering NH_4^+ from AnT-POME.

In addition to the high amount of NH_4^+, AnT-POME also contains elevated COD levels, indicating the presence of refractory organics that are resistant to biodegradation [4]. Fenton oxidation are utilized to address the COD problem. This method involves a reaction between hydrogen peroxide (H_2O_2) and ferrous ions (Fe^{2+}), which specifically target refractory compounds, thereby improving the biodegradability of wastewater within an acidic environment.

Response surface methodology (RSM) was utilized during the process optimization, along with an economic evaluation of chemical expenses. The process optimization is essential for maximizing resource utilization, minimizing the generation of undesirable side products, and ultimately enhancing its efficacy. RSM facilitates the simultaneous manipulation of multiple factors by constructing a design matrix to assess the interactions between the independent and dependent variables, aiming to optimize the conditions [6]. Furthermore, RSM offers advantages over conventional methods due to its ability to conduct faster and more systematic exploration of parameters with fewer experimental trials [7]. This study determined responses such as the removal efficiencies of NH_4^+ and soluble COD (sCOD).

Other studies have noted the presence of struvite crystals in POME, yet there is a lack of information on optimizing the factors that influence their formation. Despite the considerable sCOD concentration remaining in AnT-POME, Fenton oxidation has been applied in other studies; however, there is insufficient information on integrating struvite precipitation with Fenton oxidation for treating AnT-POME, particularly the impact of prior struvite precipitation. Considering the limited studies on struvite precipitation for NH_4^+ treatment in AnT-POME and the absence of any known studies on an integrated approach of struvite precipitation and Fenton oxidation for AnT-POME polishing treatment, our work aims to apply such an integrated approach to polish AnT-POME. In relation to this aim, the objectives were to: (i) correlate the interactions between the Mg^{2+}/NH_4^+ molar ratio, PO_4^{3-}/NH_4^+ molar ratio and pH during the optimization of struvite precipitation and (ii) strategize Fenton oxidation by optimizing parameters such as the concentration of H_2O_2,

Fe^{2+}/H_2O_2 molar ratio and reaction time, specifically for treating the supernatant obtained after struvite precipitation. The combined use of struvite precipitation for nutrient recovery and Fenton oxidation for pollution mitigation not only addresses environmental concerns but also enhances economic feasibility, establishing valuable strategies for wastewater polishing. Recovering nutrients from AnT-POME through struvite precipitation supports a circular economy by closing the nutrient loop. These recovered nutrient can be reused as fertilizers, preventing eutrophication in water bodies. Research on recycling Fenton sludge in Fenton oxidation is ongoing, aiming to enhance its feasibility [8]. Integrating these methods conserves resources, reduces waste, and promotes circular economy principles.

1.1. Struvite Precipitation

Struvite precipitation is a method used to remove and recover nutrients, specifically nitrogen and phosphorus, from wastewater. This process involves the formation of a crystalline compound known as struvite (magnesium ammonium phosphate hexahydrate, $MgNH_4PO_4 \cdot 6H_2O$), as represented by Equation (1):

$$Mg^{2+} + NH_4^{+} + PO_4^{3-} + 6H_2O \rightarrow MgNH_4PO_4 \cdot 6H_2O \quad (1)$$

This reaction depends on several factors, including pH and the concentrations of NH_4^{+}, PO_4^{3-} and Mg^{2+}. Typically, Mg^{2+} is introduced from an external chemical source and interacts with NH_4^{+} and PO_4^{3-} present in the wastewater. This process requires a supersaturation condition where the concentrations of NH_4^{+}, PO_4^{3-} and Mg^{2+} exceed their solubility product (Ksp), usually achieved under alkaline conditions within a pH range of 8–10. During supersaturation, nuclei of struvite crystals begin to form. As more ions are available, they attach to these nuclei, contributing to crystal growth. This growth continues until the ions are significantly removed from the solution or until equilibrium is reached. Unlike other precipitation processes, struvite forms relatively pure crystals with low levels of impurities and low solubility, making it easier to remove through sedimentation [9].

Numerous types of wastewater containing notably high levels of nitrogen or phosphorus, including swine wastewater, landfill leachate, and dairy wastewater, have been the focus of attention for nutrient recovery through struvite precipitation. Table 1 outlines several studies regarding the potential of struvite precipitation in removing and recovering nutrients from wastewater.

Table 1. Nutrients removal efficiency from diverse wastewater sources through struvite precipitation.

Types of Wastewater	Molar Ratio of N:P:Mg	pH	Removal Efficiency	Reference
Swine wastewater	1:1.2:1	9.0	87.96% N; 93.07% P	[10]
Landfill leachate	1:1.25:1.25	9.5	97% NH_4^{+}	[11]
Dairy wastewater	1.2:1:1.6	10.0	>89% N; >99% P	[12]

1.2. Fenton Oxidation

Fenton oxidation are utilized to address the COD problem. This method involves a reaction between hydrogen peroxide (H_2O_2) and ferrous ions (Fe^{2+}), which specifically target refractory compounds, thereby improving the biodegradability of wastewater within an acidic environment. This combination generates highly reactive hydroxyl radicals (HO•) capable of breaking down a wide range of refractory contaminants into smaller or more biodegradable molecules [13]. The chemical reactions involved in Fenton oxidation are represented as follows:

$$H_2O_2 + Fe^{2+} \rightarrow Fe^{3+} + HO\bullet + OH^{-} \quad (2)$$

$$HO\bullet + \text{organics} \rightarrow [\text{Intermediates}] \rightarrow H_2O + CO_2 \quad (3)$$

Several factors, including H_2O_2 and Fe^{2+} concentrations and reaction time, significantly influence the effectiveness of Fenton oxidation reactions. Table 2 illustrates the potential of Fenton oxidation across diverse wastewater types such as essential oil wastewater, pulp and paper wastewater, and landfill leachate in recent years, highlighting its efficiency, particularly in eliminating complex organic contaminants that pose challenges for conventional biological treatment techniques. Addressing the presence of refractory organics in POME is of paramount importance for effective wastewater treatment and environmental protection.

Table 2. COD removal efficiency from various types of wastewater through Fenton oxidation.

Types of Wastewater	H_2O_2 and Fe^{2+} Dosage	Reaction Time (min)	Removal Efficiency	Reference
Essential oil wastewater	88 mM H_2O_2; 54 mM Fe^{2+}	n.a.	81% COD	[14]
Pulp and paper wastewater	0.25 mL H_2O_2; 40 mg L^{-1} $FeSO_4$	20	84.49% COD	[15]
Landfill leachate	H_2O_2/Fe^{2+} = 1; Fe^{2+} = 3500 mg L^{-1}	120	82% COD	[16]

Note(s): n.a.: not available.

2. Materials and Methods

2.1. Wastewater and Chemicals

AnT-POME, which is the wastewater generated during palm oil milling operations, was collected after anaerobic treatment at a palm oil mill situated in Negeri Sembilan, Malaysia. This wastewater was directly employed in this study without undergoing any further filtration or dilution. Table 3 shows the properties of AnT-POME.

Table 3. Characteristics of AnT-POME.

Parameters	Average Concentration in mg L^{-1} (n = 4)
TCOD	2025 ± 106
sCOD	1370 ± 295
TN	442 ± 68
NH_4^+–N	298 ± 41
PO_4^{3-}–P	4 ± 4
Mg^{2+}	5 ± 1
TSS	613 ± 68

Magnesium chloride hexahydrate ($MgCl_2 \cdot 6H_2O$) served as Mg^{2+} source, and potassium dihydrogen phosphate (KH_2PO_4) was used as the source of PO_4^{3-} during struvite precipitation. Within Fenton's process, hydrogen peroxide (30%, H_2O_2) functioned as the oxidizing agent, while ferrous sulfate heptahydrate ($FeSO_4 \cdot 7H_2O$) acted as the catalyst. Additionally, hydrochloric acid (HCl) and sodium hydroxide solution (NaOH) were employed to regulate pH levels in both treatment processes. All chemicals used were commercially available (Sigma-Aldrich, Darmstadt, Germany and Chemiz, Shah Alam, Malaysia) and of reagent grade quality.

2.2. Design of Experiments

Experiments were conducted batch wise at ambient temperature (25 ± 2 °C). Design Expert 13.0.5 software was employed to apply central composite design (CCD), a part of RSM, for optimizing both struvite precipitation and the Fenton process, as well as evaluating the effect of three independent variables on a single response. Tables 4 and 5 illustrate the selected ranges for the independent variables, which were established following our preliminary studies and literature. In the context of struvite precipitation, Table 4 lists the independent variables, including the Mg^{2+}/NH_4^+ molar ratio (A), PO_4^{3-}/NH_4^+ molar ratio (B), and pH (C), while the response variable was $\%NH_4^+$ removal efficiency. Conversely,

for the Fenton oxidation process, Table 5 shows the independent variables, including H_2O_2 dosage in mg L^{-1} (A), Fe^{2+}/H_2O_2 molar ratio (B), and reaction time in min (C), with the %sCOD removal efficiency being the response variable of interest. Based on the CCD principle, the design involves '$2^{k'}$ fractional factorial points, '$2k$' axial points and 1 center point, where 'k' represents the number of variables (in this study, k = 3). The number of experimental runs was calculated by Equation (4) [17].

$$N = 2^k + 2k + c \quad (4)$$

Table 4. Experimental design of struvite precipitation using RSM.

Factors	Low	High	Response
Mg^{2+}/NH_4^+ molar ratio	0.8	1.4	NH_4^+ removal efficiency (%)
PO_4^{3-}/NH_4^+ molar ratio	0.8	1	
pH	7.5	8.5	

Table 5. Experimental design of Fenton oxidation using RSM.

Factors	Low	High	Response
H_2O_2 dosage (mg L^{-1})	1500	3000	sCOD removal efficiency (%)
Fe^{2+}/H_2O_2 molar ratio	0.5	1.5	
Reaction time (min)	30	60	

Here, N signifies the number of runs, k denotes the number of factors, and c represents the number of center points. In this study, a total of 20 experimental runs were conducted, incorporating diverse combinations of three variables to analyze their interactions, including 5 replications of the center point.

Subsequently, the responses were then predicted using the following quadratic model, in which Y represents the estimated response, X_i and X_j denote the independent variables, b_0 represents a constant, b_i corresponds to the linear coefficient of X_i, b_{ii} signifies the second-order effect on regression coefficients, b_{ij} is the interaction coefficient and ε denotes the statistical error [17].

$$Y = b_0 + \sum_{i=1}^{n} b_i X_i + \sum_{i=1}^{n} b_{ii} X_i^2 + \sum_{i=1}^{n} b_{ij} X_i X_j + \varepsilon \quad (5)$$

Through analysis of variance (ANOVA), coefficient of determination (R^2), Fisher's test (F test) and probability (p value) at the 95% confidence level, with an alpha of 5% ($p < 0.05$) were used to determine the interactions between the independent variables and the single dependent response, validating the model effectiveness. Contour plots were generated to visualize their interactions [17].

2.3. Struvite Precipitation

During the struvite precipitation process, pH adjustment occurred subsequent to adding the designed amounts of Mg^{2+} and PO_4^{3-} stock solutions to achieve the desired pH. The solutions were stirred for 30 min at a stirring speed of 200 rpm using a jar tester. Subsequently, the solutions were allowed to settle for 30 min to achieve struvite formation at equilibrium. The supernatants were collected for analysis and for use in subsequent Fenton's process. Table 4 lists the designed ranges of independent variables derived from a preliminary study.

2.4. Fenton Oxidation

In the Fenton process, the solutions were acidified to maintain an approximate pH value of 3 prior to being dosed with specific amounts of H_2O_2 and Fe^{2+} stock solution.

These solutions were agitated using a magnetic stirrer at a constant speed of 150 rpm for a specific duration. Following a specific stirring period, the pH was brought to approximately 7 to prevent any ongoing reactions between H_2O_2 and Fe^{2+}. The supernatants from the Fenton process were collected for analysis after 30 min of settling. Table 5 outlines the designated ranges obtained from the preliminary study for the concentration of H_2O_2, the Fe^{2+}/H_2O_2 molar ratio and reaction time.

2.5. Analytical Methods

Samples were collected at the beginning of the experiment and from the supernatant of each method (i.e., struvite precipitation and Fenton oxidation). Supernatants from struvite precipitation were filtered through a 0.2 µm syringe filter and analyzed for NH_4^+ using an 861 Advanced Compact Ion Chromatograph (Metrohm, Herisau, Switzerland). Moreover, supernatants obtained from Fenton's process were filtered through a 0.45 µm membrane filter and analyzed for soluble chemical oxygen demand (sCOD) utilizing a high range COD test kit with a DRB 200 COD digester (Hach, Loveland, CO, USA). Additionally, the solid residues acquired through struvite precipitation were characterized through field emission scanning electron microscopy (FESEM) (ZEISS SmartSEM, Oberkochen, Germany), coupled with energy-dispersive X-ray spectroscopy (EDX) (EDAX Genesis, Weiterstadt, Germany).

3. Results and Discussion

3.1. ANOVA Statistical Analysis

Figure 1 indicates that the quadratic model, along with the interactions among the independent variables and the response, exhibited statistical significance for struvite precipitation. The alignment between the observed and predicted results further validated the accuracy of the quadratic model.

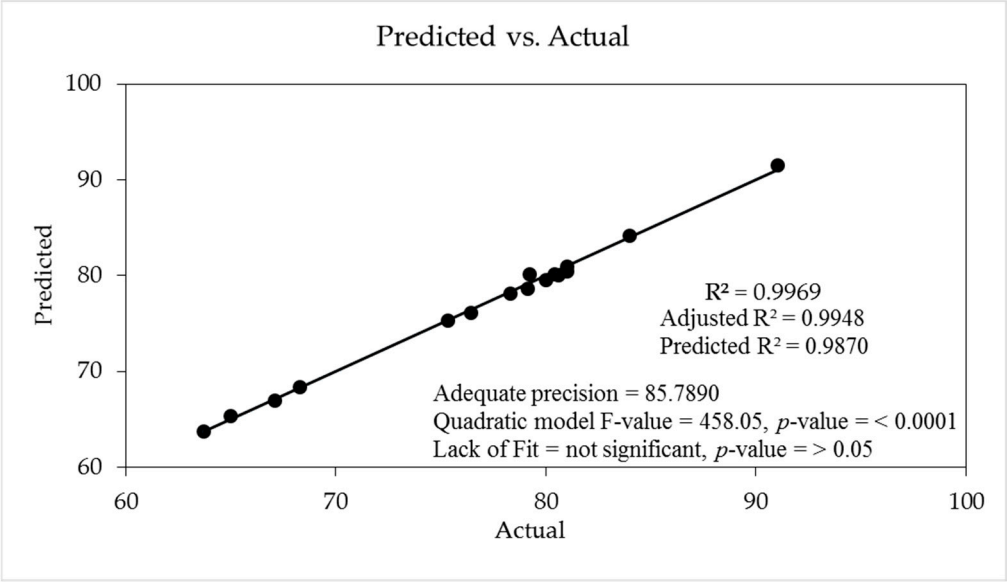

Figure 1. Predicted versus actual results with ANOVA statistics for NH4+ removal efficiency.

ANOVA was used to compare the significance and importance of the obtained model from struvite precipitation when treating AnT-POME. Figure 1 reveals that the model-F value was 458.05, with a *p*-value below 0.05. The likelihood of obtaining such a substantial F value purely by chance is only 0.01%. Additionally, the lack of fit was found to be non-significant, with a *p* value above 0.05. This highlights the substantial predictive capacity of the model. Moreover, the coefficient of determination (R^2 = 0.9969) indicated that the model could accurately predict the correlation between the independent variables (namely, the Mg^{2+}/NH_4^+ molar ratio, PO_4^{3-}/NH_4^+ molar ratio and pH) and the response (NH_4^+ removal efficiency). Furthermore, the predicted R^2 closely corresponds to the adjusted

R^2, with values of 0.9870 and 0.9948, respectively. The adjusted R^2 is employed to assess the goodness-of-fit for models with varying numbers of independent variables, whereas the predicted R^2 evaluates the model's predictive capability. In addition, the adequate precision, which involves comparing the range of the predicted values at the design points to the average prediction error, was assessed. A value exceeding 4 is an indication of adequate model discrimination according to StatEase Design-Expert 13.0.5 software. In this study, the precision was 85.789, significantly surpassing the threshold of 4. All these suggested that the struvite precipitation's model was well suited for exploring the design space as defined by the CCD.

Table 6 presents the individual terms for the Mg^{2+}/NH_4^+ molar ratio, PO_4^{3-}/NH_4^+ molar ratio, and pH, all showing statistical significance in relation to NH_4^+ removal efficiency, with their p values less than 0.05. Further, the squared terms for the Mg^{2+}/NH_4^+ molar ratio and pH also demonstrate significance, indicating a non-linear relationship between these factors and the response. Furthermore, the significance of interaction terms such as Mg^{2+}/NH_4^+ molar ratio with PO_4^{3-}/NH_4^+ molar ratio, Mg^{2+}/NH_4^+ molar ratio with pH, and PO_4^{3-}/NH_4^+ molar ratio with pH suggested that the influence of one factor on the response depends on the levels of other factors. Therefore, both main effects and interaction effects need to be considered in interpreting the results. To refine the model, non-significant variables can be excluded based on their lack of association with the response variable [18].

Table 6. ANOVA analysis of quadratic model for NH4+ removal efficiency.

Source	F-Value	*p*-Value	Remarks
Quadratic Model	187.10	<0.0001	significant
A: Mg^{2+}/NH_4^+ molar ratio	380.49	<0.0001	
B: PO_4^{3-}/NH_4^+ molar ratio	134.84	<0.0001	
C: pH	5.54	0.0382	
AB	75.19	<0.0001	
AC	6.90	0.0235	
BC	3.55	0.0862	
A^2	76.69	<0.0001	
C^2	762.61	<0.0001	
Lack of Fit	0.2943	0.9157	not significant

Note(s): A, B, and C represent the independent factors in struvite precipitation.

Equation (6), expressed in terms of the actual factors for NH_4^+ removal efficiency (Y_1), is as follows:

$$Y_1 = -1395.484 + 78.981A + 27.999B + 349.474C - 76.875AB - 4.658AC + 10.025BC + 18.504A^2 - 22.023C^2 \quad (6)$$

Here, A represents the Mg^{2+}/NH_4^+ molar ratio, B represents the PO_4^{3-}/NH_4^+ molar ratio, and C denotes pH. Notably, this modified model was used to predict the optimum conditions for struvite precipitation with synergistic effects illustrated with positive values, while negative values for opposing effects [7].

In the case of Fenton oxidation, considering the interaction effects of the concentration of H_2O_2, Fe^{2+}/H_2O_2 molar ratio, and reaction time on the sCOD removal efficiency, Figure 2 illustrates that the data were fitted to a quadratic model. This fit was deemed significant based on the F value of 165.92 and a p value below 0.05. The lack of fit was not statistically significant compared to the pure error, indicating that the model fit the data effectively. The R^2 value of 0.989 implies that approximately 98.9% of the variability in sCOD removal efficiency can be attributed to the experimental variables under investigation. Furthermore, the adjusted and predicted R^2 values, which are 0.9812 and 0.9691, respectively, are reasonably consistent.

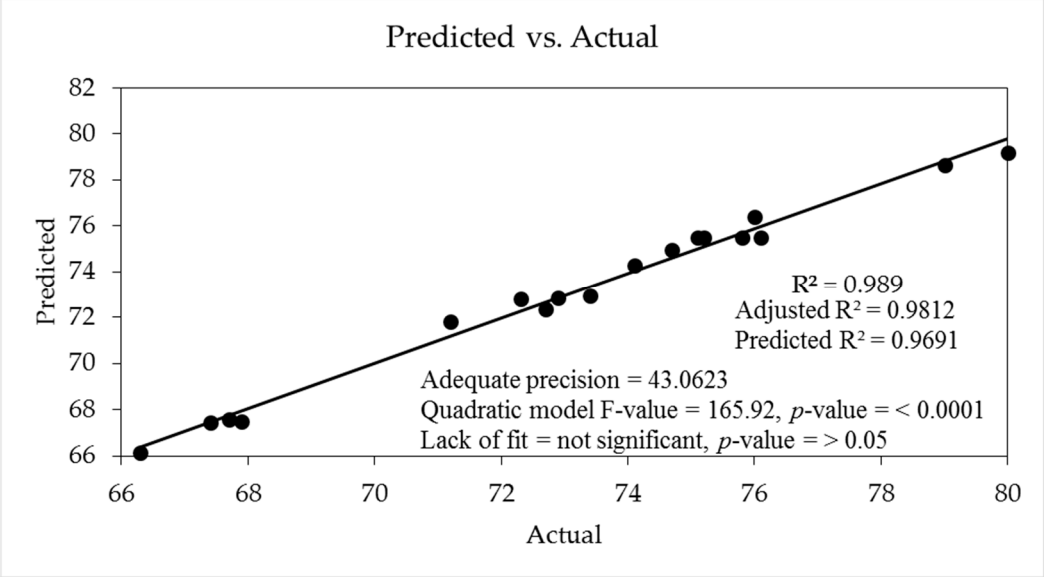

Figure 2. Predicted versus actual results with ANOVA statistics for sCOD removal efficiency.

Table 7 illustrates the results of ANOVA analysis for the model terms of Fenton oxidation. The results indicated that the H_2O_2 dosage, molar ratio of Fe^{2+}/H_2O_2, and reaction time were highly statistical significance ($p < 0.05$). Additionally, the interaction terms between H_2O_2 dosage and the molar ratio of Fe^{2+}/H_2O_2, as well as between H_2O_2 dosage and reaction time, along with the quadratic term for the molar ratio of Fe^{2+}/H_2O_2 also demonstrated significance.

Table 7. ANOVA analysis for sCOD model.

Source	F-Value	*p*-Value	Remarks
Quadratic Model	165.92	<0.0001	significant
A: H_2O_2 dosage (mg L^{-1})	251.66	<0.0001	
B: Fe^{2+}/H_2O_2 molar ratio	7.71	0.0157	
C: Reaction time (min)	183.19	<0.0001	
AB	3.74	0.0751	
AC	19.55	0.0007	
B^2	529.69	<0.0001	
Lack of Fit	1.32	0.3955	not significant

Note(s): A, B, and C represent the independent factors in Fenton oxidation.

Equation (7) in terms of the actual factors affecting sCOD removal efficiency (Y_2), is as follows:

$$Y_2 = 45.11 + 0.005A + 23.264B + 0.285C + 0.001AB - 0.00007AC - 12.298B^2 \quad (7)$$

Here, A represents the H_2O_2 dosage, B represents the molar ratio of Fe^{2+}/H_2O_2, and C denotes the reaction time. This modified equation could be employed as a valuable tool for forecasting the optimum conditions for Fenton oxidation.

Moreover, Figure 3 shows the residual analysis results derived from model fitting and the perturbation plot generated through ANOVA regression during struvite precipitation. Notably, Figure 3a demonstrates a symmetrical distribution of residual data points around the red line, indicating the reliability of the regression model obtained from CCD analysis in accurately predicting responses during NH_4^+ removal performance simulation. Figure 3b displays a random scatter of residuals around the mean value, suggesting their independence from the run order and falling within the red control boundaries. These

analyses, based on residual analysis, collectively affirmed the adequacy of the model in describing NH_4^+ removal performance through struvite precipitation [19].

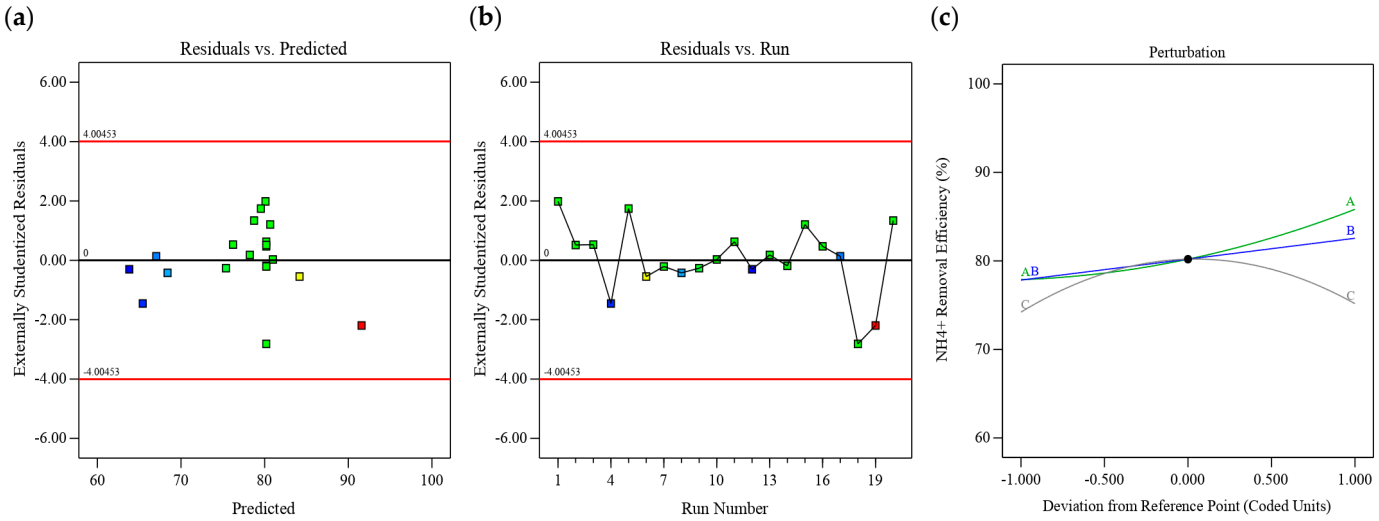

Figure 3. Design expert plot (**a**) residuals versus predicted; (**b**) residual versus run; (**c**) perturbation plot illustrating the effects of A: Mg^{2+}/NH_4^+ molar ratio, B: PO_4^{3-}/NH_4^+ molar ratio and C: pH for NH_4^+ removal efficiency data. Note(s): blue color shows the lowest predicted value in legend range; green/yellow color shows the middle predicted value in legend range; red color shows the highest predicted value in legend range.

Figure 3c displays the perturbation plot for NH_4^+ removal from AnT-POME through struvite precipitation. This plot serves as a tool for assessing the impact of all factors on the response at a specific point within the design space. The perturbation plot depicts how the response changes as each factor deviates from a chosen reference point. The lower, middle and upper levels of the factors are denoted by −1, 0, and +1, respectively, where A is the Mg^{2+}/NH_4^+ molar ratio, B is the PO_4^{3-}/NH_4^+ molar ratio and C is the pH. The reference point for the perturbation plot was set at the midpoint (0 value). A positive curvature signifies that the response increases with increasing factor level, while a negative curvature indicates that the response decreases with increasing factor level [20].

From Figure 3c, both the Mg^{2+}/NH_4^+ molar ratio and pH exhibited pronounced and similar curvature, albeit with opposing effects on NH_4^+ removal efficiency, indicating that the corresponding response was highly sensitive to these factors. This observation agrees well with Wu et al.'s [21] findings, who emphasized the significant influence of the Mg^{2+} concentration on the degree of supersaturation. Moreover, a broad pH range can support struvite precipitation, but the suitable pH range varies for different wastewater types. In addition, Equation (8) indicates that the pH is a crucial factor for struvite precipitation [22]. Therefore, adjusting the pH was found to have a detrimental effect on NH_4^+ removal efficiency.

$$Mg^{2+} + NH_4^+ + HPO_4^{2-} + 6H_2O \rightarrow MgNH_4PO_4{\cdot}6H_2O + H^+ \quad (8)$$

On the other hand, Figure 4a,b portray the residual analysis of the model for Fenton oxidation, with all plots meeting satisfactory standards. All the data points fell within the red boundaries, indicating a high level of confidence in the model's reliability and accuracy in predicting the sCOD removal efficiency during Fenton oxidation. Additionally, Figure 4c illustrates the perturbation plot, depicting the influence of the H_2O_2 concentration, Fe^{2+}/H_2O_2 molar ratio and reaction time at a specific point within the design space. The pronounced curvature observed in the Fe^{2+}/H_2O_2 molar ratio suggests that this factor greatly influences sCOD removal efficiency, making it the most critical factor compared to

H_2O_2 dosage and reaction time. Nonetheless, its negative curvature has the opposite effect on the sCOD removal efficiency when increasing the Fe^{2+} dosage.

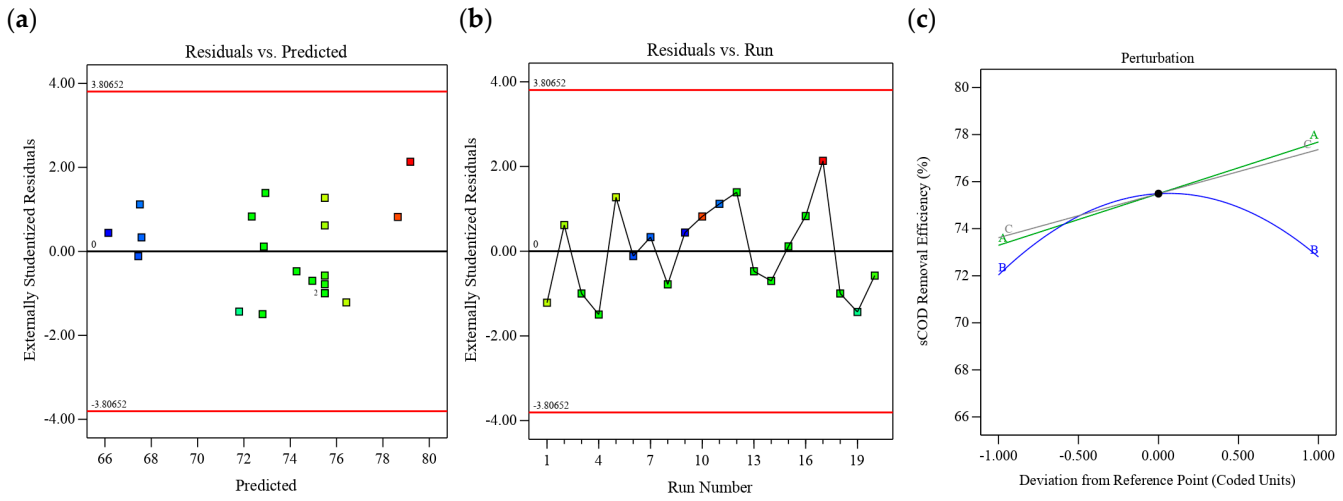

Figure 4. Design expert plot depicts (**a**) residuals versus predicted; (**b**) residual versus run; (**c**) perturbation plot demonstrating the effects of H_2O_2 dosage (A), Fe^{2+}/H_2O_2 molar ratio (B) and reaction time (C) on sCOD removal efficiency. Note(s): blue color shows the lowest predicted value in legend range; green/yellow color shows the middle predicted value in legend range; red color shows the highest predicted value in legend range.

3.2. Struvite Precipitation: The Influence of Variables

AnT-POME was polished through struvite precipitation. Figure 5 presents the response surface plots used to analyze the effects of each variable (i.e., molar ratios of Mg^{2+}/NH_4^+ and PO_4^{3-}/NH_4^+ as well as pH) and their interactions during struvite precipitation. According to the preliminary study and other relevant research, these three factors had more pronounced effects on the precipitation process with a relatively short reaction time of 30 min when supersaturation was achieved [23]. In addition, as indicated in Equation (8), the presence of Mg^{2+}, PO_4^{3-}, and NH_4^+ and the pH are the crucial factors for struvite precipitation [22].

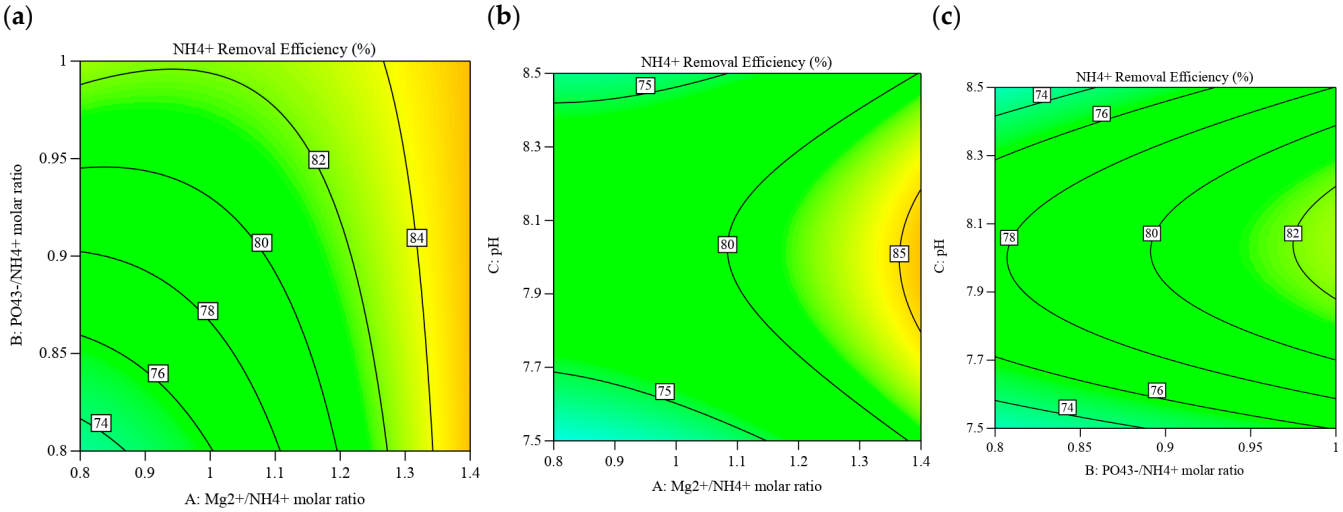

Figure 5. Contour plots illustrating the interactions between (**a**) Mg^{2+}/NH_4^+ and PO_4^{3-}/NH_4^+ molar ratios, (**b**) Mg^{2+}/NH_4^+ molar ratio and pH, and (**c**) PO_4^{3-}/NH_4^+ molar ratio and pH in relation to NH_4^+ removal efficiency.

3.2.1. Interactions between the Mg^{2+}/NH_4^+ Molar Ratio and PO_4^{3-}/NH_4^+ Molar Ratio

As shown in Figure 5a, the efficiency of NH_4^+ removal exhibited a direct correlation with the molar ratios of Mg^{2+}/NH_4^+ and PO_4^{3-}/NH_4^+. Crystallization occurs when the solution reaches a state of supersaturation with respect to struvite, marked by the ion activity products of the three constituent ions (i.e., Mg^{2+}, NH_4^+ and PO_4^{3-}) surpassing their respective solubility products [24]. As the dosage of Mg^{2+} and PO_4^{3-} increased, the concentration of dissolved ions surpassed their equilibrium values, leading to favorable conditions for precipitation. This observation underscores the direct relationship between struvite saturation and the logarithm of the ionic concentration within the crystal [24].

Furthermore, Figure 5a demonstrates that having an excess of Mg^{2+} (i.e., >1) proved highly advantageous for enhancing NH_4^+ removal efficiency. Huang and Liu [25] reported that in addition to struvite, various magnesium phosphate precipitates, such as $Mg(H_2PO_4)_2$, $MgHPO_4$, $Mg_3(PO_4)_2$ or $Mg(OH)_2$ can form. On the other hand, in this study, the molar ratio of PO_4^{3-}/NH_4^+ was maintained below an excess value. This precaution aimed to avoid accumulation at the end of the reaction, as such accumulation could precipitate with the subsequent Fenton process. Specifically, there is a chance of precipitation occurring with Fe^{2+}, a crucial component required for Fenton oxidation [26].

3.2.2. Interactions between Mg^{2+}/NH_4^+ Molar Ratio or PO_4^{3-}/NH_4^+ Molar Ratio with pH

The pH range crucial for struvite precipitation varies depending on the type of wastewater. Struvite typically forms at pH levels between 8 to 10. Precipitation occurs during supersaturation, which necessitates an increase in pH, reducing the solubility of Mg^{2+}, NH_4^+, and PO_4^{3-}. When the concentrations of these ions surpass the solubility product (K_{sp}) of struvite, nuclei begin to form. The solubility product of struvite is given by:

$$K_{sp} = [Mg^{2+}]\,[NH_4^+]\,[PO_4^{3-}]$$

As the pH increases (pH 8–10), it promotes the dissociation of NH_4^+ and PO_4^{3-}, enhancing their availability. Once nuclei form, they serve as sites for further growth. The growth process involves the continuous attachment of Mg^{2+}, NH_4^+, and PO_4^{3-} from the solution onto the crystal surface [9].

Figure 5b, c illustrate the influence of both the Mg^{2+}/NH_4^+ and PO_4^{3-}/NH_4^+ molar ratios on NH_4^+ removal efficiency was dependent on the pH. Slight pH adjustments (pH 8.1 $\pm$ 0.2) occurred as the Mg^{2+}/NH_4^+ and PO_4^{3-}/NH_4^+ molar ratios increased. This indicated in our work, fewer chemical dosages for pH adjustments were needed to facilitate struvite formation, given that the initial AnT-POME pH was 7.9 $\pm$ 0.5. This finding was aligned with Chen et al.'s [27] study, which demonstrated struvite precipitation in anaerobically treated swine wastewater was under slightly alkaline conditions (i.e., pH 7–8). Increasing the dose of Mg^{2+} ions can contribute to a decreased dependence on pH adjustment. This is because Mg^{2+} serves as a pH buffer and is capable of reacting with hydroxide ions to generate alkaline compounds such as magnesium hydroxide, effectively stabilizing the pH without the need for supplementary pH-adjusting agents [28]. It is crucial, however, to carefully monitor and regulate the Mg^{2+} dosage to avoid exceeding the desired pH range or causing unwanted precipitation of compounds that may interfere with the treatment process.

Figure 5b,c also demonstrates that at the lowest pH (pH 7.5), the removal efficiency of NH_4^+ remained low due to the increased solubility of struvite, making the precipitation of struvite less likely [29]. Moreover, Hao et al. [30] argued that struvite precipitation occurs in the presence of HPO_4^{2-} rather than PO_4^{3-}, as indicated in Equation (8). At lower pH (acidic conditions), an excess of H^+ ions is present in the solution due to a higher concentration of free protons. According to Equation (9), HPO_4^{2-} ions can interact with H^+ ions, resulting in the formation of $H_2PO_4^-$. Consequently, this process leads to a reduction in the concentration of HPO_4^{2-} ions, and thus limits their availability for the struvite

precipitation reaction. Therefore, in an acidic environment, fewer HPO_4^{2-} ions react with Mg^{2+} and NH_4^+ ions, impeding the formation of struvite crystals [27].

$$HPO_4^{2-} + H^+ \rightarrow H_2PO_4^- \quad (9)$$

Similarly, a lower NH_4^+ removal efficiency was observed when the pH surpassed 8.3. This observation was attributed to the predominant formation of $Mg_3(PO_4)_2$ and $Mg(OH)_2$ salts instead of struvite, as reported by Huang and Liu [25]. Ogata et al. [31] also discussed the higher affinity of Mg^{2+} for PO_4^{3-} ions. Therefore, in the case of AnT-POME, when the pH of the solution is maintained at a moderate level, approximately 8, it becomes conducive for the formation of a struvite precipitate ($MgNH_4PO_4 \cdot 6H_2O$).

Following struvite precipitation, the concentrations of NH_4^+-N and TN in AnT-POME decreased from 298 ± 41 mg L^{-1} and 442 ± 68 mg L^{-1} to 44 ± 0.1 mg L^{-1} and 93 ± 3.1 mg L^{-1}, respectively. This suggests successful removal and recovery of NH_4^+-N through struvite precipitation, leading to a decrease in TN. However, sCOD, which could not be removed through struvite precipitation, remained at a high concentration (1360 ± 330 mg L^{-1}). Consequently, AnT-POME was subsequently subjected to Fenton oxidation for further treatment.

3.3. Fenton Oxidation: The Influence of Variables

Collected supernatant from struvite precipitation was subsequently treated by Fenton oxidation for the removal of sCOD. This wastewater contained a relatively high concentration of sCOD (i.e., an average 1350 mg L^{-1} sCOD) which contributed to its brownish appearance. It is important to note that the PO_4^{3-} residual concentration in the collected supernatant was nearly negligible at 0 mg L^{-1}, thus posing no adverse effect on the Fenton process [26]. RSM was employed to optimize the performance of Fenton oxidation for treating the collected supernatant from struvite precipitation, considering factors derived from preliminary study and other research that indicated interaction effects among dosage of H_2O_2, molar ratio of Fe^{2+}/H_2O_2 and reaction time. The dosage of the oxidizing agent (H_2O_2) and catalyst (Fe^{2+}) as well as the reaction time for the completion of the Fenton's process are contingent upon the wastewater strength [32]. Figure 6 presents the 2D contour plots of the sCOD removal efficiency through the Fenton reaction, illustrating the interaction effect between the independent variables on the response.

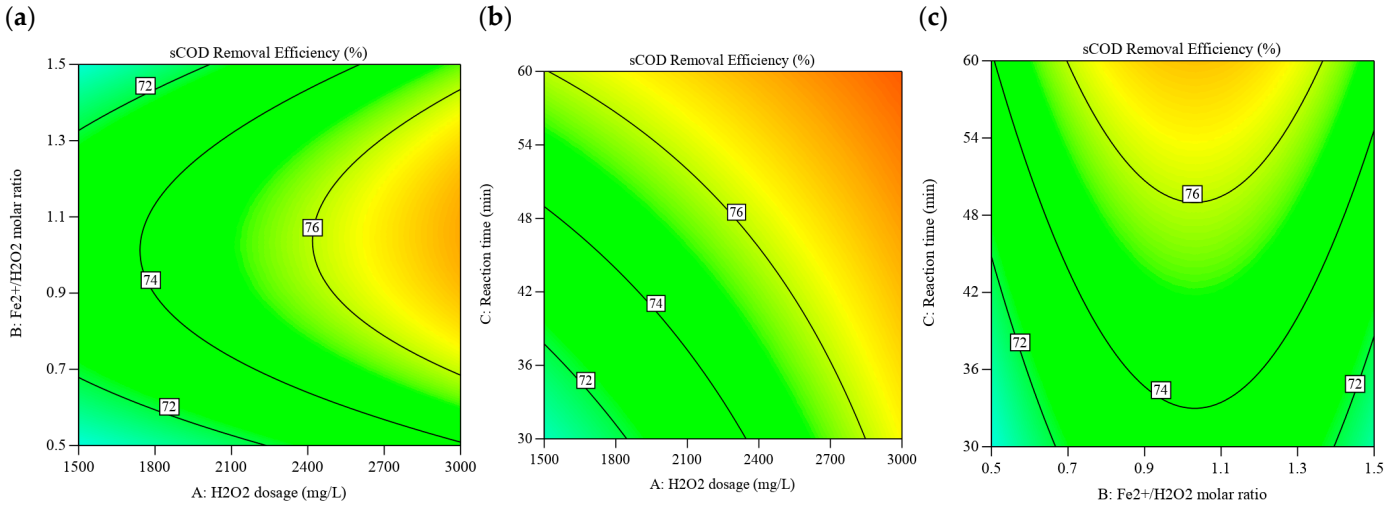

Figure 6. Contour plots depict the interrelationships between (**a**) H_2O_2 dosage and Fe^{2+}/H_2O_2 molar ratio, (**b**) H_2O_2 dosage and reaction time, and (**c**) Fe^{2+}/H_2O_2 molar ratio and reaction time with respect to sCOD removal efficiency.

3.3.1. Interactions between H_2O_2 Dosage with Molar Ratio of Fe^{2+}/H_2O_2

Figure 6a shows that the Fenton reaction involves the reaction between H_2O_2 and Fe^{2+} to generate hydroxyl radicals (HO•), a highly reactive species capable of oxidizing refractory pollutants. These HO• effectively oxidizes refractory pollutants into several intermediates, such as organic acids, subsequently improving the biodegradability of refractory pollutants [13]. The efficiency of sCOD removal was observed to increase proportionally with the H_2O_2 dosage. When the H_2O_2 dosage increased, within the Fe^{2+}/H_2O_2 molar ratio range of 0.7–1.4, a significant amount of H_2O_2 was decomposed and generated a greater quantity of HO•, consequently contributing to an elevated rate of sCOD oxidation. Conversely, a lower dosage of H_2O_2 resulted in fewer HO• being produced, thus limiting the reaction efficiency.

Moreover, the interaction between H_2O_2 and Fe^{2+} was interdependent. Figure 6a demonstrates that increasing H_2O_2 concentration necessitated adjusting the Fe^{2+}/H_2O_2 molar ratio to maintain the efficient production of HO•. A higher Fe^{2+}/H_2O_2 molar ratio accelerated H_2O_2 decomposition and increased the production of HO•. However, Figure 6a,c demonstrate that excessively high molar ratios reduced efficiency. For instance, at an H_2O_2 dosage of 1800 mg L^{-1}, Fe^{2+}/H_2O_2 molar ratios of 1 and 1.5 resulted in 74.1% and 71.5% sCOD removal efficiency, respectively. This was attributed to the elevated amount of Fe^{2+}, which had a negative impact, as it scavenged hydroxyl radicals, leading to the formation of ferric hydroxide sludge, as shown in Equation (10) [11,22]. Furthermore, Equation (11) shows that the generated Fe^{3+} from Fenton oxidation could react with H_2O_2, resulting in the generation of another radicals, namely hydroperoxyl radicals (HO_2•) [11,33]. Equation (12) indicates that the presence of HO_2• also had the capacity to scavenge OH• radicals, leading to a reduced sCOD removal efficiency [11,33]. Moreover, HO_2• may actively degrade organic compounds, albeit with lower reactivity and a longer time required [34]. This is because HO_2• has a lower standard potential redox value (1.77 V) than H_2O_2 (2.8 V) [13]. Therefore, achieving an optimal balance between H_2O_2 dosage and Fe^{2+}/H_2O_2 molar ratio is crucial to maximize the production of HO• without significant scavenging effects.

$$HO\bullet + Fe^{2+} \rightarrow Fe^{3+} + OH^- \quad (10)$$

$$Fe^{3+} + H_2O_2 \rightarrow Fe^{2+} + H^+ + HO_2\bullet \quad (11)$$

$$HO_2\bullet + OH\bullet \rightarrow O_2 + H_2O \quad (12)$$

3.3.2. Interactions between H_2O_2 Dosage or Molar Ratio of Fe^{2+}/H_2O_2 with Reaction Time

Figure 6b,c illustrate that with an extended reaction time, there will be a sufficient opportunity for OH• production and the subsequent oxidation of refractory organic substances. It is important to note that the reaction time showed a positive correlation with the sCOD removal efficiency. In this context, extended periods of time provided sufficient time for the Fe^{2+} and H_2O_2 reactions to generate OH•, thus enhancing the efficiency of sCOD removal.

Figure 7 displays the changes in color following Fenton oxidation, showing that the successful reduction in sCOD was responsible for the brownish appearance [35]. As discussed earlier, an increase in H_2O_2 dose is correlated with improved sCOD removal efficiency. However, Figure 7 also demonstrates that an excess Fe^{2+}/H_2O_2 molar ratio at a higher H_2O_2 dosage can result in ferrous hydroxide sludge formation, causing brown turbidity in the wastewater [13]. Additionally, an extended reaction time contributed to increased oxidation and thus higher sCOD removal efficiency with a more transparent appearance. However, Figure 7 shows that there is a notable concern regarding the generation of Fenton sludge at the conclusion of the reaction.

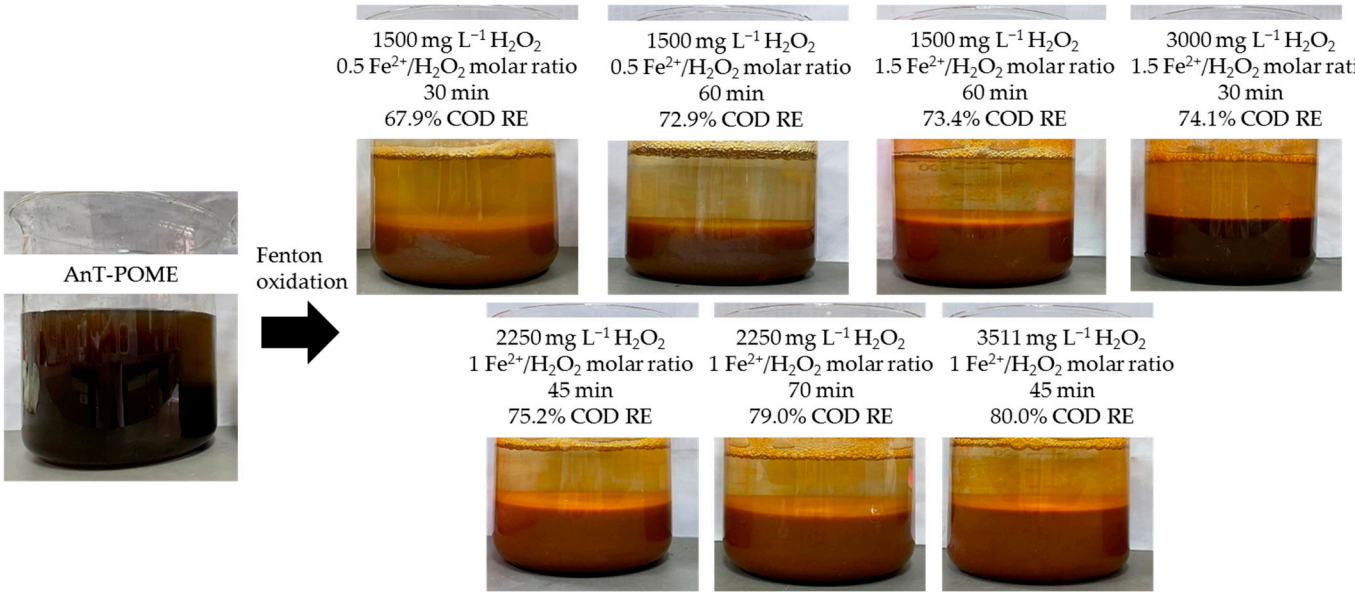

Figure 7. Changes in color following Fenton oxidation (RE: removal efficiency).

3.4. Optimization and Model Validation

The optimal parameters for both struvite precipitation and Fenton oxidation were determined through numerical optimization using a desirability function set to 1. Optimized conditions were those with lower chemical dosages within the constrained condition range determined from response surface models, while achieving higher pollutants removal efficiency. For the struvite precipitation process, the optimum conditions involved a Mg^{2+}/NH_4^+ molar ratio and a PO_4^{3-}/NH_4^+ molar ratio both at 1, and the pH was 8.2. On the other hand, the optimum conditions for Fenton oxidation were determined to be H_2O_2 concentration of 2680 mg L^{-1}, a Fe^{2+}/H_2O_2 molar ratio of 0.8, and a reaction duration of 56 min.

As discussed in Section 3.3, both the struvite precipitation and Fenton oxidation models demonstrated strong R^2 values of up to 0.9, indicating a robust correlation between the predicted and actual values. This finding was further supported by Table 8, which summarizes the experimental errors—less than 5% between the predicted and actual removal efficiencies at optimized conditions, indicating the reliability of the quadratic model derived from RSM. Nonetheless, even slight variations in experimental measurements can significantly impact large-scale applications by influencing prediction accuracy, operational costs, and adherence to regulatory standards. Therefore, future research should scale up based on the identified impact factors from this study and their optimization, aiming for a comprehensive evaluation of treatment efficiency goals, regulatory compliance and economic impacts.

Table 9 provides an overview of the characteristics of AnT-POME following polishing treatment with struvite precipitation and Fenton oxidation. The final effluent met the discharge standard limits for POME, where nutrient, such as NH_4^+, and refractory organics, such as sCOD, present in AnT-POME were effectively removed. Furthermore, when comparing our proposed alternative methods with conventional biological treatment, it became evident that the integration of struvite precipitation and Fenton oxidation exhibited superior efficiency in removing refractory pollutants and made effective use of valuable nutrients present in the anaerobically treated wastewater. This advancement contributes to the prospect for nutrient recovery and promotes environmental sustainability.

Table 10 also demonstrates the removal performance of current and proposed polishing technologies. In this study, the integration of struvite precipitation and Fenton oxidation exhibited better removal performance than coagulation but lower removal performance compared to membrane technology and the combination of sequencing batch reactor and

adsorption. While membrane technology achieves the highest COD removal, its treatment cost can be prohibitive [4]. On the other hand, adsorption, using agricultural biomass, can be an economical polishing method, but its reusability is low and it is energy-intensive due to the regeneration process and secondary waste disposal [36,37]. Coagulation, often combined with other methods, faces concerns regarding sludge recycling after treatment [37]. Considering these factors, the integration of struvite precipitation and Fenton oxidation effectively mitigates environmental pollution and is cost effective in recovering existing resource in wastewater. There have also been investigations into recycling Fenton sludge as a coagulant, adsorbent, and source of Fe^{2+} [8].

Table 8. Model validation under optimum conditions.

Treatment Method	Optimum Conditions	Predicted Removal Efficiency	Actual Removal Efficiency	Error (%)
Struvite precipitation	Mg^{2+}/NH_4^+ molar ratio: 1; PO_4^{3-}/NH_4^+ molar ratio: 1; pH: 8.2	81.8% NH_4^+	78.8 ± 1.6% NH_4^+	3.7
Fenton oxidation	H_2O_2 dosage: 2680 mg L^{-1}; Fe^{2+}/H_2O_2 molar ratio: 0.8; Reaction time: 56 min	77.1% sCOD	76.0 ± 1.0% sCOD	1.1

Table 9. Comparison between conventional treatment and proposed methods in relation to discharge standards.

	TCOD	sCOD	NH_4^+-N
AnT-POME	2025 ± 106	1350 ± 336	298 ± 41
Effluent after **anaerobic treatment + struvite precipitation + Fenton oxidation** (this study)	313 ± 39	308 ± 46	41 ± 7.1
Effluent after **anaerobic + aerobic treatment** [38–40]	768 ± 242	n.a.	44 ± 44
Standard Discharge Limit (Department Of Environment (Malaysia), 1984) [41]	400	n.a.	150

Note(s): n.a.: not available. Units in mg L^{-1}.

Table 10. Comparison of removal performance between proposed and current polishing technologies.

Treatment Methods	Removal Performance
Anaerobic treatment + struvite precipitation + Fenton oxidation (this study)	76.0% COD 78.8% NH_4^+ 67.1% TN
Anaerobic treatment + coagulation [42]	69% COD 52% NH_4^+
Anaerobic treatment + membrane technology [4]	100% TOC 84% TN
Anaerobic treatment + sequencing batch reactor + adsorption [43]	98.3% COD 98.3% NH_4^+

3.4.1. Characterization of Struvite Precipitate from AnT-POME

The struvite precipitate was derived from AnT-POME under optimal conditions (a Mg^{2+}/NH_4^+ molar ratio of 1, a PO_4^{3-}/NH_4^+ molar ratio of 1 and a pH of 8.2). The collected precipitate was subjected to FESEM and EDX analyses. Figure 8 shows that the morphology of the precipitate closely matched that of the orthorhombic structure, confirming its identity as a struvite crystal. However, the FESEM images also revealed the presence of additional precipitates alongside struvite. Figure 9 displays the EDX analysis, revealing an elemental molar ratio of P:N:Mg at 1:0.5:0.9, with corresponding weight percentages of 17.68%, 4.29% and 13.19%, respectively. The elevated ratios of P and Mg to N could be attributed to the

formation of other precipitates, such as $MgHPO_4$, $MgHPO_4 \cdot 3H_2O$, $Mg(PO_3OH) \cdot 3H_2O$, $Mg_3(PO_4)_2$, $Mg_3(PO_4)_2 \cdot 22H_2O$, $Mg_3(PO_4)_2 \cdot 8H_2O$, and $Mg_2P_2O_7$, as noted by Huang and Liu [25].

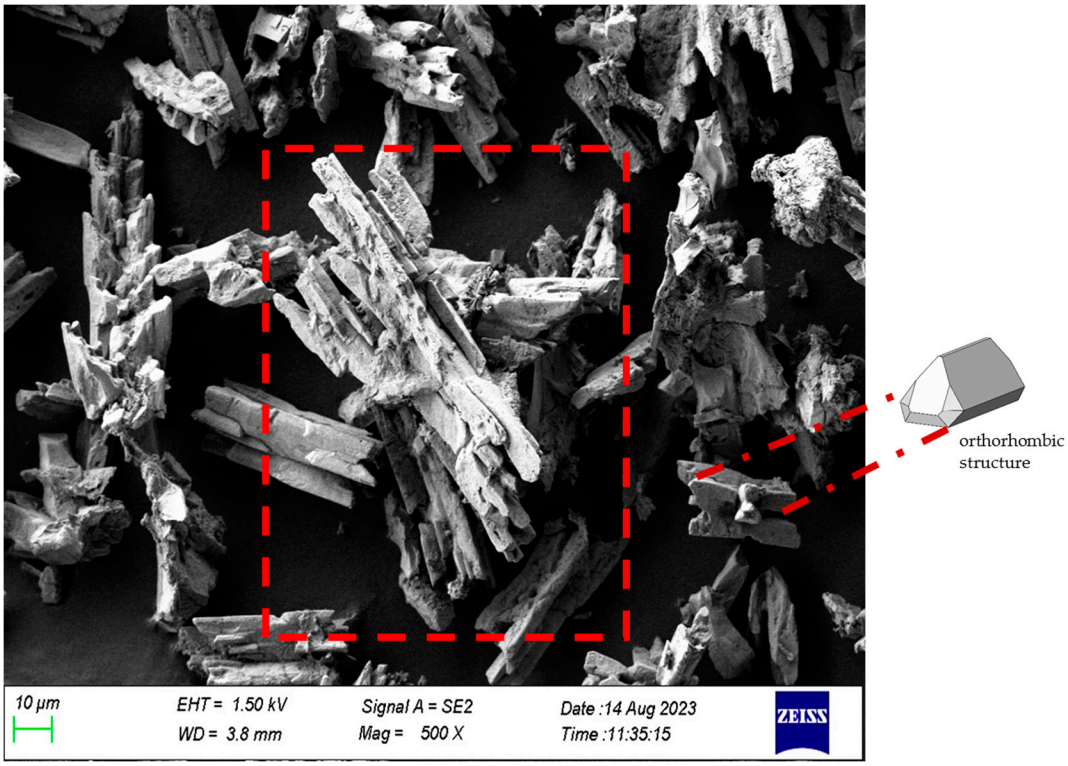

Figure 8. Morphology and orthorhombic structure of struvite crystals formed during the precipitation process.

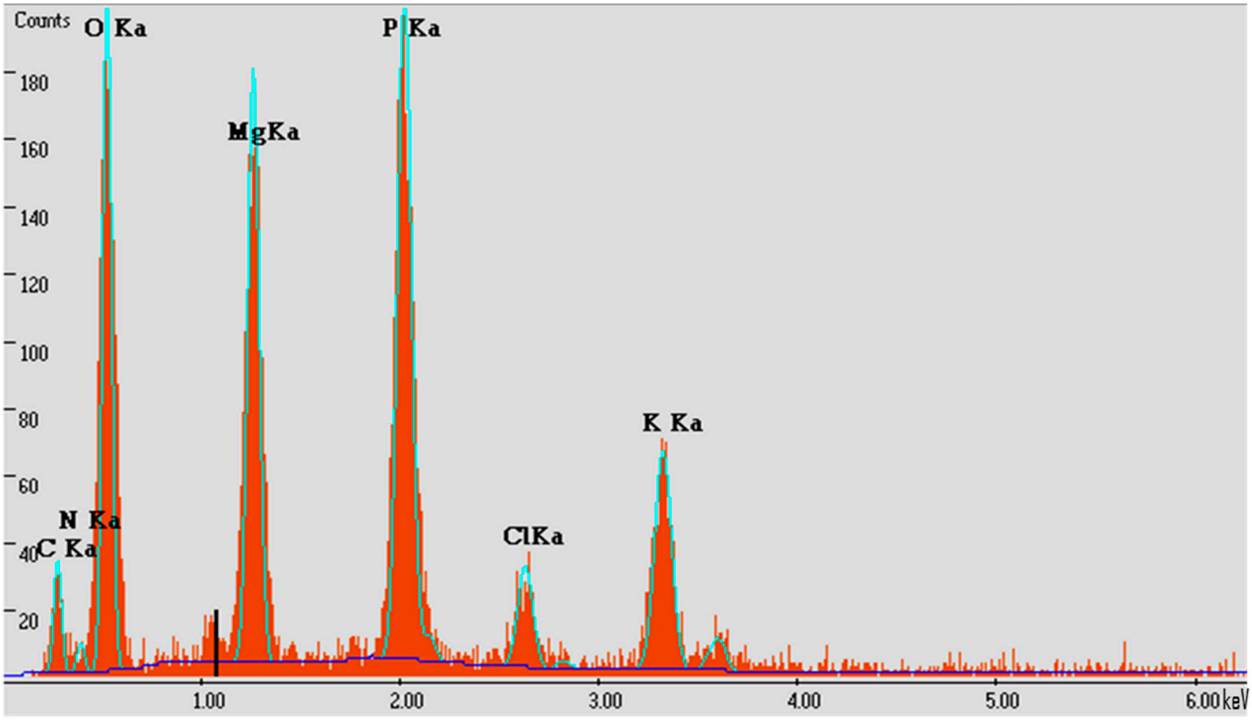

Figure 9. EDX analysis about the elemental composition of red box labelled struvite crystals in Figure 8.

3.4.2. Economic Assessment of Chemical Costs

The economic assessment herein focused solely on the expenses associated with the chemicals used. It did not encompass the costs of energy consumption or the commercial value of recovered struvite crystals. Table 11 presents the comprehensive chemical costs for removing 1 kg of NH_4^+, with the optimum conditions involving a Mg^{2+}/NH_4^+ molar ratio of 1, a PO_4^{3-}/NH_4^+ molar ratio of 1, and a pH adjustment of 8.2. The cost for $MgCl_2{\cdot}6H_2O$, supplying Mg^{2+}, was 0.15 USD kg^{-1}, while KH_2PO_4, providing PO_4^{3-}, was 0.40 USD kg^{-1}. Consequently, the total treatment cost was 5.66 USD kg^{-1}-average removed NH_4^+.

Table 11. Chemical cost analyses for integrated struvite precipitation and Fenton oxidation at optimum conditions.

Characterization of Final Effluent after Anaerobic Treatment + Struvite Precipitation + Fenton Oxidation (mg L^{-1})	Optimum Conditions of Struvite Precipitation	Mg^{2+} Cost (USD kg^{-1}-Average Removed NH_4^+)	PO_4^{3-} Cost (USD kg^{-1}-Average Removed NH_4^+)	Total Chemicals Cost (USD kg^{-1}-Average Removed NH_4^+)
TCOD: 313 ± 39 sCOD: 308 ± 46 TSS: 350 ± 28 VSS: 43 ± 13 TN: 72 ± 7.7 NH_4^+-N: 41 ± 7.1 PO_4^{3-}-P: ~0	(i) Mg^{2+}/NH_4^+ molar ratio: 1; (ii) PO_4^{3-}/NH_4^+ molar ratio: 1; (iii) pH: 8.2	2.03	3.63	5.66
	Optimum conditions of Fenton Oxidation	**Fe^{2+} cost (USD kg^{-1}-average removed sCOD)**	**H_2O_2 cost (USD kg^{-1}-average removed sCOD)**	**Total chemicals cost (USD kg^{-1}-average removed sCOD)**
	(i) H_2O_2 dosage: 2680 mg L^{-1} (ii) Fe^{2+}/H_2O_2 molar ratio: 0.8 (iii) Reaction time: 56 min	0.13	2.11	2.24

Note(s): $MgCl_2{\cdot}6H_2O$ unit price of 0.15 USD kg^{-1}; KH_2PO_4 unit price of 0.4 USD kg^{-1}; $FeSO_4{\cdot}7H_2O$ unit price of 0.03 USD kg^{-1}; 30%, H_2O_2 unit price of 0.49 USD kg^{-1}.

Table 11 also details the chemical expenses associated with the Fenton process, using the USD kg^{-1} of average removed sCOD. The cost of $FeSO_4{\cdot}7H_2O$ was considered to be 0.03 USD kg^{-1}, while the cost of 30% H_2O_2 was 0.49 USD kg^{-1}. The optimal operational parameters for Fenton oxidation were determined to be 2680 mg L^{-1} H_2O_2 and a Fe^{2+}/H_2O_2 molar ratio of 0.8. Therefore, the total chemical cost of removing up to 79% of the sCOD was 2.24 USD kg^{-1}-average removed sCOD.

The economic expenses associated with struvite precipitation and Fenton oxidation are primarily influenced by the cost of technical grade chemical reagents. Cost savings in chemical procurement can be achieved through the use of more affordable chemical sources. For example, utilizing H_3PO_4 as a PO_4^{3-} source, employing MgO as a Mg^{2+} source (possibly obtained from the byproduct of magnesite calcination, as suggested by Perwitasari et al. [44]), and recycling ferric sludge as a source of Fe^{2+} are viable strategies. In addition, a significant concern arises regarding the production of ferric sludge following the Fenton process. Shi et al. [45] observed that by recycling the extracted Fe^{2+} from residual sludge, comparable performance to that of commercial $FeSO_4$ could be achieved. This cyclic utilization approach has the potential to reduce costs by more than 60% and promote zero-waste discharge.

3.5. Challenges and Future Perspectives

Stringent environmental regulations are now in place, promoting the widespread adoption of circular economy principles in wastewater treatment. To ensure that the final effluent complies with regulatory discharge standards, the use of efficient polishing technologies is needed. This study demonstrated the potential of combining struvite precipitation and Fenton oxidation for polishing AnT-POME. Although this experimentation

occurred at the laboratory scale, there is a critical need to comprehend and optimize these proposed treatment processes for scaling up in practical applications.

Some challenges were observed throughout the experiment. For instance, the dosage of chemical in both struvite precipitation and Fenton oxidation. Exceeding a certain threshold or adding an excess of PO_4^{3-} could result in accumulation, leading to further precipitation with Fe^{2+} in subsequent Fenton's process and influencing sCOD removal. In addition, the presence of TSS in AnT-POME led to agglomeration with struvite, potentially altering the struvite morphology and purity. The use of struvite precipitation as a polishing treatment following anaerobic process and sedimentation can effectively prevent TSS from adhering to the surface of the precipitate. Additionally, the scarcity of Mg^{2+} in wastewater poses a significant challenge because it results in high chemical costs for the treatment process, given that Mg^{2+} is a crucial component of struvite formation. An interesting alternative is the utilization of natural Mg^{2+} resources, such as bittern or industrial wastewater that is rich in Mg^{2+}, such as metal processing wastewater, paper and pulp industry wastewater, and textile industry wastewater. Such use of Mg^{2+} obtained from these resources could help reduce the cost of chemicals required [9].

On the other hand, the management of iron-based sludge, a byproduct of the Fenton process, raises considerable concerns regarding proper disposal. Some researchers have explored the potential of repurposing this sludge to address the limitations of Fenton oxidation. For example, Shi et al. [45] studied the in situ cyclic utilization of Fe^{2+} from Fe^{3+} sludge for Fenton oxidation, achieving comparable performance to the commercial Fe^{2+} chemical source with zero waste discharge. In addition, Gao et al. [8] reviewed that Fe^{3+} sludge could be recycled as a coagulant, reducing disposed sludge by up to 50% and simultaneously decreasing coagulant usage by 50%. Wang et al. [46] introduced iron-rich biochar pyrolyzed from Fe^{3+} sludge to adsorb P, where the recovered P was reused as a fertilizer, thus fulfilling the principles of circular economy. These findings demonstrate efforts to mitigate secondary pollution by utilizing Fe^{3+} sludge as a source of iron, coagulant and adsorbent.

Overall, the application of integrated struvite precipitation and Fenton oxidation as polishing treatment has demonstrated its potential for recovering nutrients and removing refractory organics from AnT-POME. Therefore, future research should direct efforts to explore more effective avenues for reducing treatment costs. Notably, in this study, AnT-POME was treated without sterilization, potentially allowing for microbial activity that could contribute to the removal of NH_4^+ and sCOD [47]. In future studies, a comparison of pollutant removal performance between sterilized and non-sterilized AnT-POME could be conducted to further explore the impact of microbial activity on the integrated struvite precipitation and Fenton oxidation process.

4. Conclusions

This study aimed to assess NH_4^+ removal and recovery through struvite precipitation, as well as sCOD removal through Fenton oxidation from AnT-POME. The experimental work utilized RSM and ANOVA analysis to analyze the interaction effects of operational factors and optimize them. NH_4^+ removal efficiency was found to depend on the pH and Mg^{2+}/NH_4^+ molar ratio. Mg^{2+}/NH_4^+ molar ratio facilitates precipitation with PO_4^{3-}, preventing accumulation for subsequent Fenton oxidation and acting as a pH buffer, which reduces the need for pH adjustment. On the other hand, the treatment efficiency of sCOD was primarily influenced by the Fe^{2+}/H_2O_2 molar ratio. Furthermore, the precision of the response surface models for both struvite precipitation and Fenton oxidation was evident, as reflected by high R^2 values. Under the optimum conditions for struvite precipitation (equimolar ratio of NH_4^+:PO_4^{3-}:Mg^{2+} and a pH of 8.2), NH_4^+ removal efficiency achieved 78.8 ± 1.6%. For Fenton oxidation, with a Fe^{2+}/H_2O_2 molar ratio of 0.8, a H_2O_2 dosage of 2680 mg L^{-1}, and a reaction time of 56 min, 76.0 ± 1.0% sCOD removal efficiency was reached. Therefore, this study underscores the effectiveness of RSM in experimental design and highlights the promising approach of integrating struvite precipitation and Fenton

oxidation for polishing POME, providing simultaneous removal and recovery of nutrients, along with the efficient elimination of refractory organics responsible for pollution.

Author Contributions: Conceptualization, Y.F.S., M.F.R. and A.S.M.C.; methodology, Y.F.S.; software, Y.F.S.; validation, Y.F.S.; formal analysis, Y.F.S.; investigation, Y.F.S.; resources, M.F.R. and A.S.M.C.; data curation, Y.F.S.; writing—original draft preparation, Y.F.S.; writing—review and editing, M.F.R., A.S.M.C. and G.C.N.; visualization, M.F.R., A.S.M.C. and G.C.N.; supervision, M.F.R. and A.S.M.C.; project administration, M.F.R.; funding acquisition, M.F.R. All authors have read and agreed to the published version of the manuscript.

Funding: This work was supported by the Universiti Malaya (UM) RU Geran—Fakulti Program (GPF059B-2020) and UM International Collaboration Grant (ST045-2022).

Institutional Review Board Statement: Not applicable.

Informed Consent Statement: Not applicable.

Data Availability Statement: Data are contained within the article.

Acknowledgments: The authors would like to thank Kamal Fawwaz and Tang Kar Huey for facilitating sampling activities throughout the duration of this study. We also greatly appreciate the assistance from Loi Jia Xing and Leong Chew Lee with laboratory analysis.

Conflicts of Interest: The authors declare no conflict of interest.

References

1. MPOC Malaysian Palm Oil Industry–MPOC. Available online: https://mpoc.org.my/malaysian-palm-oil-industry/ (accessed on 4 January 2022).
2. Cheng, Y.W.; Chong, C.C.; Lam, M.K.; Ayoub, M.; Cheng, C.K.; Lim, J.W.; Yusup, S.; Tang, Y.; Bai, J. Holistic Process Evaluation of Non-Conventional Palm Oil Mill Effluent (POME) Treatment Technologies: A Conceptual and Comparative Review. *J. Hazard. Mater.* **2021**, *409*, 124964. [CrossRef]
3. Yacob, S.; Hung, Y.-T.; Shirai, Y.; Ali Hassan, M. Treatment of Palm Oil Wastewaters. *Waste Treat. Food Process. Ind.* **2005**, *7*, 101–117. [CrossRef]
4. Bello, M.M.; Abdul Raman, A.A. Trend and Current Practices of Palm Oil Mill Effluent Polishing: Application of Advanced Oxidation Processes and Their Future Perspectives. *J. Environ. Manag.* **2017**, *198*, 170–182. [CrossRef]
5. Abdullah, M.F.; Md Jahim, J.; Abdul, P.M.; Mahmod, S.S. Effect of Carbon/Nitrogen Ratio and Ferric Ion on the Production of Biohydrogen from Palm Oil Mill Effluent (POME). *Biocatal. Agric. Biotechnol.* **2020**, *23*, 101445. [CrossRef]
6. Shim, S.; Won, S.; Reza, A.; Kim, S.; Ahmed, N.; Ra, C. Design and Optimization of Fluidized Bed Reactor Operating Conditions for Struvite Recovery Process from Swine Wastewater. *Processes* **2020**, *8*, 422. [CrossRef]
7. Faraj, H.; Jamrah, A.; Al-Omari, S.; Al-Zghoul, T.M. Optimization of an Electrocoagulation-Assisted Adsorption Treatment System for Dairy Wastewater. *Case Stud. Chem. Environ. Eng.* **2024**, *9*, 100574. [CrossRef]
8. Gao, L.; Cao, Y.; Wang, L.; Li, S. A Review on Sustainable Reuse Applications of Fenton Sludge during Wastewater Treatment. *Front. Environ. Sci. Eng.* **2022**, *16*, 77. [CrossRef]
9. Siciliano, A.; Limonti, C.; Curcio, G.M.; Molinari, R. Advances in Struvite Precipitation Technologies for Nutrients Removal and Recovery from Aqueous Waste and Wastewater. *Sustainability* **2020**, *12*, 7538. [CrossRef]
10. Ha, T.H.; Mahasti, N.N.N.; Lu, M.C.; Huang, Y.H. Ammonium-Nitrogen Recovery as Struvite from Swine Wastewater Using Various Magnesium Sources. *Sep. Purif. Technol.* **2023**, *308*, 122870. [CrossRef]
11. Rayshouni, H.; Wazne, M. Effects of Calcium on the Removal of Ammonium from Aged Landfill Leachate by Struvite Precipitation. *Water* **2022**, *14*, 1993. [CrossRef]
12. Gong, W.; Li, Y.; Luo, L.; Luo, X.; Cheng, X.; Liang, H. Application of Struvite-MAP Crystallization Reactor for Treating Cattle Manure Anaerobic Digested Slurry: Nitrogen and Phosphorus Recovery and Crystal Fertilizer Efficiency in Plant Trials. *Int. J. Environ. Res. Public Health* **2018**, *15*, 1397. [CrossRef] [PubMed]
13. Riadi, L.; Miracle, T.; Hartawati, M. Fenton Degradation of Lignin Wastewater in a Batch Process for Pulp and Paper Industry: Kinetic and Economic Aspect. *Int. J. Eng. Technol.* **2019**, *11*, 1102–1107. [CrossRef]
14. Akgül, S.T. Investigation of the Treatability of Essential Oil Industry Wastewater Using Fenton Oxidation Process. *Desalin. Water Treat.* **2022**, *267*, 52–61. [CrossRef]
15. Javeed, T.; Nawaz, R.; Al-Hussain, S.A.; Irfan, A.; Irshad, M.A.; Ahmad, S.; Zaki, M.E.A. Application of Advanced Oxidation Processes for the Treatment of Color and Chemical Oxygen Demand of Pulp and Paper Wastewater. *Water* **2023**, *15*, 1347. [CrossRef]
16. De Carluccio, M.; Fiorentino, A.; Rizzo, L. Multi-Barrier Treatment of Mature Landfill Leachate: Effect of Fenton Oxidation and Air Stripping on Activated Sludge Process and Cost Analysis. *J. Environ. Chem. Eng.* **2020**, *8*, 104444. [CrossRef]

17. Wong, L.P.; Isa, M.H.; Bashir, M.J.K. Disintegration of Palm Oil Mill Effluent Organic Solids by Ultrasonication: Optimization by Response Surface Methodology. *Process Saf. Environ. Prot.* **2018**, *114*, 123–132. [CrossRef]
18. Minitab Interpret the Key Results for Analyze Taguchi Design. Available online: https://support.minitab.com/en-us/minitab/help-and-how-to/statistical-modeling/doe/how-to/taguchi/analyze-taguchi-design/interpret-the-results/key-results/ (accessed on 6 June 2024).
19. Tang, Y.M.; Tan, K.T.; Wong, L.P. Valorization of Palm Oil Mill Effluent via Enhanced Oil Recovery as an Alternative Feedstock for Biodiesel Production. *Water Sci. Technol.* **2023**, *88*, 1404–1416. [CrossRef]
20. Faggiano, A.; De Carluccio, M.; Cerrato, F.; Garcia Junior, C.A.; Proto, A.; Fiorentino, A.; Rizzo, L. Improving Organic Matter and Nutrients Removal and Minimizing Sludge Production in Landfill Leachate Pre-Treatment by Fenton Process through a Comprehensive Response Surface Methodology Approach. *J. Environ. Manag.* **2023**, *340*, 117950. [CrossRef] [PubMed]
21. Wu, J.; Li, Y.; Xu, B.; Li, M.; Wang, J.; Shao, Y.; Chen, F.; Sun, M.; Liu, B. Effects of Physicochemical Parameters on Struvite Crystallization Based on Kinetics. *Int. J. Environ. Res. Public Health* **2022**, *19*, 7204. [CrossRef] [PubMed]
22. Wang, F.; Fu, R.; Lv, H.; Zhu, G.; Lu, B.; Zhou, Z.; Wu, X.; Chen, H. Phosphate Recovery from Swine Wastewater by a Struvite Precipitation Electrolyzer. *Sci. Rep.* **2019**, *9*, 8893. [CrossRef]
23. Taddeo, R.; Lepistö, R. Struvite Precipitation in Raw and Co-Digested Swine Slurries for Nutrients Recovery in Batch Reactors. *Water Sci. Technol.* **2015**, *71*, 892–897. [CrossRef] [PubMed]
24. Song, W.; Li, Z.; Liu, F.; Ding, Y.; Qi, P.; You, H.; Jin, C. Effective Removal of Ammonia Nitrogen from Waste Seawater Using Crystal Seed Enhanced Struvite Precipitation Technology with Response Surface Methodology for Process Optimization. *Environ. Sci. Pollut. Res.* **2018**, *25*, 628–638. [CrossRef]
25. Huang, A.H.; Liu, J.C. Removal of Ammonium as Struvite from Wet Scrubber Wastewater. *Water. Air. Soil Pollut.* **2014**, *225*, 2062. [CrossRef]
26. Su, C.C.; Chen, C.M.; Anotai, J.; Lu, M.C. Removal of Monoethanolamine and Phosphate from Thin-Film Transistor Liquid Crystal Display (TFT-LCD) Wastewater by the Fluidized-Bed Fenton Process. *Chem. Eng. J.* **2013**, *222*, 128–135. [CrossRef]
27. Chen, R.F.; Liu, T.; Rong, H.W.; Zhong, H.T.; Wei, C.H. Effect of Organic Substances on Nutrients Recovery by Struvite Electrochemical Precipitation from Synthetic Anaerobically Treated Swine Wastewater. *Membranes* **2021**, *11*, 594. [CrossRef] [PubMed]
28. Campbell, B. What Is Magnesium Hydroxide? Available online: https://www.wwdmag.com/what-is-articles/article/21004707/what-is-magnesium-hydroxide (accessed on 4 June 2024).
29. González-Morales, C.; Fernández, B.; Molina, F.J.; Naranjo-Fernández, D.; Matamoros-Veloza, A.; Camargo-Valero, M.A. Influence of Ph and Temperature on Struvite Purity and Recovery from Anaerobic Digestate. *Sustainability* **2021**, *13*, 10730. [CrossRef]
30. Hao, X.D.; Wang, C.C.; Lan, L.; Van Loosdrecht, M.C.M. Struvite Formation, Analytical Methods and Effects of PH and Ca^{2+}. *Water Sci. Technol.* **2008**, *58*, 1687–1692. [CrossRef]
31. Ogata, F.; Uematsu, Y.; Fukuda, M.; Saenjum, C.; Kabayama, M.; Nakamura, T.; Kawasaki, N. Changes in the Mechanism of the Reaction between Phosphate and Magnesium Ions: Effect of Initial Concentration and Contact Time on Removal of Phosphate Ions from Aqueous Media. *J. Environ. Chem. Eng.* **2020**, *8*, 104385. [CrossRef]
32. USP Technologies Fentons Reagent General Chemistry Using H_2O_2. Available online: https://usptechnologies.com/fentons-reagent-general-chemistry-using-h2o2/ (accessed on 5 February 2024).
33. Saeed, M.O.; Azizli, K.; Isa, M.H.; Bashir, M.J.K. Application of CCD in RSM to Obtain Optimize Treatment of POME Using Fenton Oxidation Process. *J. Water Process Eng.* **2015**, *8*, e7–e16. [CrossRef]
34. Gamaralalage, D.; Sawai, O.; Nunoura, T. Degradation Behavior of Palm Oil Mill Effluent in Fenton Oxidation. *J. Hazard. Mater.* **2019**, *364*, 791–799. [CrossRef] [PubMed]
35. Zahrim, A.Y.; Nasimah, A.; Hilal, N. Pollutants Analysis during Conventional Palm Oil Mill Effluent (POME) Ponding System and Decolourisation of Anaerobically Treated POME via Calcium Lactate-Polyacrylamide. *J. Water Process Eng.* **2014**, *4*, 159–165. [CrossRef]
36. Chai, W.S.; Cheun, J.Y.; Kumar, P.S.; Mubashir, M.; Majeed, Z.; Banat, F.; Ho, S.H.; Show, P.L. A Review on Conventional and Novel Materials towards Heavy Metal Adsorption in Wastewater Treatment Application. *J. Clean. Prod.* **2021**, *296*, 126589. [CrossRef]
37. Yashni, G.; Al-Gheethi, A.; Radin Mohamed, R.M.S.; Arifin, S.N.H.; Mohd Salleh, S.N.A. Conventional and Advanced Treatment Technologies for Palm Oil Mill Effluents: A Systematic Literature Review. *J. Dispers. Sci. Technol.* **2020**, *42*, 1766–1784. [CrossRef]
38. Norhan, M.A.; Abdullah, S.R.S.; Hasan, H.A.; Ismail, N.I. A Constructed Wetland System for Bio-Polishing Palm Oil Mill Effluent and Its Future Research Opportunities. *J. Water Process Eng.* **2021**, *41*, 102043. [CrossRef]
39. Sa'at, S.K.M.; Zaman, N.Q.; Yusoff, M.S. Effect of Hydraulic Retention Time on Palm Oil Mill Effluent Treatment in Horizontal Sub-Surface Flow Constructed Wetland. In Proceedings of the 6th International Conference on Environment (ICENV2018): Empowering Environment and Sustainable Engineering Nexus through Green Technology, Penang, Malaysia, 11–13 December 2018; Volume 2124.
40. Sa'at, S.K.M.; Zaman, N.Q. Suitability of Ipomoea Aquatica for the Treatment of Effluent from Palm Oil Mill. *J. Built Environ. Technol. Eng.* **2017**, *2*, 39–44.
41. Department of Environment Ministry of Natural Resources and Environmental Sustainability Environmental Quality Act 1974 [ACT 127]. Available online: https://www.doe.gov.my/environmental-quality-prescribed-premises-crude-palm-oil-amendment-regulations-1982-p-u-a-183-82/ (accessed on 9 May 2024).

42. Saad, M.S.; Wirzal, M.D.H.; Putra, Z.A. Review on Current Approach for Treatment of Palm Oil Mill Effluent: Integrated System. *J. Environ. Manag.* **2021**, *286*, 112209. [CrossRef] [PubMed]
43. Farraji, H.; Mohammadpour, R.; Zaman, N.Q. Post-Treatment of Palm Oil Mill Effluent Using Zeolite and Wastewater. *J. Oil Palm Res.* **2021**, *33*, 103–118. [CrossRef]
44. Perwitasari, D.S.; Muryanto, S.; Jamari, J.; Bayuseno, A.P. Optimization of Struvite Crystallization and Heavy Metal Recovery in Wastewater Using Response Surface Methodology. *Orient. J. Chem.* **2018**, *34*, 336–345. [CrossRef]
45. Shi, L.; Zhang, Y.; Zeng, C.; Lai, X.; Chen, S. Zero Sludge Discharge Strategy for Fenton Oxidation Wastewater Treatment Technology: Biological Regeneration and in-Situ Cyclic Utilization—A Feasibility Study. *J. Clean. Prod.* **2022**, *376*, 134259. [CrossRef]
46. Wang, H.; Xiao, K.; Yang, J.; Yu, Z.; Yu, W.; Xu, Q.; Wu, Q.; Liang, S.; Hu, J.; Hou, H.; et al. Phosphorus Recovery from the Liquid Phase of Anaerobic Digestate Using Biochar Derived from Iron−rich Sludge: A Potential Phosphorus Fertilizer. *Water Res.* **2020**, *174*, 115629. [CrossRef] [PubMed]
47. Wang, Z.; Gao, M.; She, Z.; Jin, C.; Zhao, Y.; Yang, S.; Guo, L.; Wang, S. Effects of Hexavalent Chromium on Performance and Microbial Community of an Aerobic Granular Sequencing Batch Reactor. *Environ. Sci. Pollut. Res.* **2015**, *22*, 4575–4586. [CrossRef] [PubMed]